Protein Expression and Purification 22, 174–179 (2001)
doi:10.1006/prep.2001.1422, available online at http://www.idealibrary.com on IDEAL®

High-Level Soluble Production and Characterization of Porcine Ribonuclease Inhibitor

Tony A. Klink,* Anna M. Vicentini,† Jan Hofsteenge,†,[1] and Ronald T. Raines*,‡,[1]

Department of Biochemistry and ‡Department of Chemistry, University of Wisconsin–Madison, Madison, Wisconsin 53706; and †Friedrich Miescher-Institut, CH-4002 Basel, Switzerland

Received September 29, 2000, and in revised form February 14, 2001; published online May 21, 2001

Ribonucleases can be cytotoxic if they retain their ribonucleolytic activity in the cytosol. The cytosolic ribonucleolytic activity of ribonuclease A (RNase A) and other pancreatic-type ribonucleases is limited by the presence of excess ribonuclease inhibitor (RI). RI is a 50-kDa cytosolic scavenger of pancreatic-type ribonucleases that competitively inhibits their ribonucleolytic activity. RI had been overproduced as inclusion bodies, but its folding *in vitro* is inefficient. Here, porcine RI (pRI) was overproduced in *Escherichia coli* using the *trp* promoter and minimal medium. This expression system maintains pRI in the soluble fraction of the cytosol. pRI was purified by affinity chromatography using immobilized RNase A and by anion-exchange chromatography. The resulting yield of 15 mg of purified RI per liter of culture represents a 60-fold increase relative to previously reported recombinant DNA systems. Differential scanning calorimetry was used to study the thermal denaturation of pRI, RNase A, and the pRI–RNase A complex. The conformational stability of the complex is greater than that of the individual components.

Ribonuclease inhibitor (RI)[2] is a 50-kDa scavenger of pancreatic-type ribonucleases. RI binds pancreatic-type ribonucleases with 1:1 stoichiometry and competitively inhibits their ribonucleolytic activity (1–3). RI is found in the cytosol of mammalian cells and has been purified from many species and tissue types (4, 5). Its inhibition of ribonucleolytic activity and its cytosolic location has led to the suggestion that RI protects cellular RNA from degradation by invading pancreatic-type ribonucleases (3).

Ribonucleases can be cytotoxic by entering the cytosol and degrading cellular RNA. Although bovine pancreatic ribonuclease (RNase A (6); EC 3.1.27.5) has high ribonucleolytic activity (6) and is capable of entering the cytosol (7), its ribonucleolytic activity there is limited by the presence of excess RI (3, 8). The noncovalent interactions of the RI–RNase A complex are exceptionally strong ($K_d = 6.7 \times 10^{-14}$ M (9)). Homologous ribonucleases are able to evade inhibition by RI (10, 11). Indeed, Onconase, which is a homolog of RNase A from the Northern leopard frog (*Rana pipiens*), has $>10^8$-fold lower affinity for RI than does RNase A and is cytotoxic (12).

The amino acid residues of RI homologs from pig, cow, sheep, mouse, rat, and human are conserved to >70% (4). Each RI homolog consists of 15 leucine-rich repeats, which are common in proteins that are involved in protein–protein interactions (13–20). Another unusual aspect of the RI sequence is the presence of a large number, 30 in porcine RI (pRI), of highly conserved cysteine residues (21). Each cysteine residue must be reduced for binding to ribonucleases. Consequently, oxidation of these residues is detrimental to inhibition of ribonucleolytic activity (21, 22). This feature allows RI to function only in a reducing environment, such as the cytosol.

RI is a horseshoe-shaped protein that engulfs ribonucleases (Fig. 1). Of the 124 residues in RNase A, 24

[1] To whom correspondence may be addressed. E-mail: hofsteenge@fmi.ch or raines@biochem.wisc.edu.

[2] Abbreviations used: CNBr, cyanogen bromide; DSC, differential scanning calorimetry; DTT, dithiothreitol; 6-FAM, 6-carboxyfluorescein; 6-TAMRA, 6-carboxytetramethylrhodamine; LB, Luria–Bertani; Mes, 2-(*N*-morpholino)ethanesulfonic acid; PAGE, polyacrylamide gel electrophoresis; PDB, protein data bank; Pipes, 1,4-piperazine diethane sulfonic acid; PMSF, phenylmethylsulfonyl fluoride; pRI, porcine ribonuclease inhibitor; RI, ribonuclease inhibitor; RNase A, bovine pancreatic ribonuclease A; SDS, sodium dodecyl sulfate; Tris, tris(hydroxymethyl)aminomethane.

1046-5928/01 $35.00

FIG. 1. Structure of the complex between porcine ribonuclease inhibitor and ribonuclease A. Ribbon diagrams were created with programs MOLSCRIPT (37) and RASTER3D (38) by using coordinates derived from X-ray diffraction analysis (PDB entry 1DFJ (16)).

are within 4 Å of pRI in the pRI–RNase A complex. RI is an acidic protein (pI = 4.7 (19)). Accordingly, its binding to ribonucleases, which are basic (pI > 9.0 (23–25)), likely has a Coulombic component (2, 19). Angiogenin, an RNase A homolog, also binds tightly to RI ($K_i = 7.1 \times 10^{-16}$ M (2)). Yet, different intermolecular contacts are made by RI in binding RNase A and angiogenin (20, 26, 27).

Elucidating the interactions of RI and ribonucleases could enhance understanding of tight protein–protein interactions. Unfortunately, biophysical studies are made problematic by the difficulty of isolating RI from natural sources (4, 5). Likewise, inclusion bodies have been produced when RI is produced in *Escherichia coli*. The requirement for reduced cysteine residues complicates RI folding *in vitro*, with one system yielding only 0.25 mg of RI per liter of culture (28).

Here, we report expression of pRI. Our system uses the *trp* promoter and minimal medium. With this system, pRI remains in the cytosol and is maintained in the soluble fraction during cell lysis. The yield of pRI from this expression and purification system is 60-fold higher than any reported previously. This high yield enabled us to perform biophysical experiments on pRI as well as the pRI-RNase A complex.

EXPERIMENTAL PROCEDURES

Materials

Escherichia coli strain TOPP 3 (Rif^r [F′ *proAB lacI*^{q}ZΔ*M15* Tn10 (Tet^r) (Kan^r)]), which is a non-K-12 strain, was from Stratagene (La Jolla, CA). RNase A used in the calorimetric assays was a generous gift from P. A. Leland. RNasin (which is human RI) and all enzymes for the manipulation of DNA were from Promega (Madison, WI). SDS–PAGE molecular weight standards were from Bio-Rad Laboratories (Hercules, CA). Phenylmethylsulfonyl fluoride (PMSF), and 2-(*N*-morpholino)ethanesulfonic acid (Mes) were from Sigma Chemical Company (St. Louis, MO). The fluorogenic RNase A substrate 6-FAM–(dA)rU(dA)$_2$–6-TAMRA was from Integrated DNA Technologies (Coralville, IA) (29). 1,4-Piperazine diethane sulfonic acid (Pipes) was from Fisher Biotech (Fair Lawn, NJ). Cyanogen bromide (CNBr)-activated Sepharose Fast Flow lab pack and the HiTrap Q column were from Amersham Pharmacia Biotech (Piscataway, NJ). M9 minimal salts (5×), Bacto yeast extract, and Bacto peptone were from Difco Laboratories (Detroit, MI).

Luria–Bertani (LB) medium contained (in 1.00 L) Bacto tryptone (10 g), Bacto yeast extract (5 g), and NaCl (10 g). Pipes M9 minimal medium contained (in 1.00 L) 7.1 mM Pipes–NaOH buffer (pH 8.0), M9 minimal salts (1×), K_2HPO_4 (36.8 mM), NH_4Cl (3.0 mM), K_2SO_4 (2.4 mM), $CaCl_2$ (0.07 mM), $MgCl_2$ (1.0 mM), glycerol (0.64% v/v), and Tween 20 (0.05% v/v). All media were prepared in distilled, deionized water and autoclaved. All other chemicals were of reagent grade or better and were used without further purification unless indicated otherwise.

Analytical Instruments

Ultraviolet and visible absorbance measurements were made with a Cary 3 double-beam spectrophotometer equipped with a Cary temperature controller from Varian (Sugar Land, TX). Calorimetry experiments were performed with an MCS differential scanning calorimeter from MicroCal (Northampton, MA). Fluorescence measurements were made with a QuantaMaster1 photon counting fluorometer from Photon Technology International (South Brunswick, NJ) equipped with sample stirring. The concentration of purified pRI was determined by using $\varepsilon = 0.88$ mL mg^{-1} cm^{-1} at 280 nm (30). The concentration of RNase A was determined by using $\varepsilon = 0.72$ mL mg^{-1} cm^{-1} at 277.5 nm (31). The concentration of the RI–RNase A complex was determined by using $\varepsilon = 0.86$ mL mg^{-1} cm^{-1} at 280 nm (30). The concentration of 6-FAM–(dA)rU(dA)$_2$–6-TAMRA was determined by using $\varepsilon = 102{,}400$ M^{-1} cm^{-1} at 260 nm (29).

Methods

Design and construction of plasmid pTrpmRI6.1. The active form of pRI contains 30 reduced cysteine residues (21). To prevent the oxidation of the cysteine residues and thereby produce pRI in a soluble state,

we designed plasmid pTrpmRI6.1 to maintain the protein in the reducing environment of the cytosol. DNA encoding the pRI gene (9) was cloned into plasmid pHR 148 (32). An *Eco*RI restriction site was incorporated into the 3′ end and a *Bam*HI restriction site was incorporated into the 5′ end of the pRI gene by the polymerase chain reaction (33). The resulting plasmid, pTrpmRI6.1, carries a cDNA encoding pRI with its expression controlled by the *trp* promoter.

Production and purification of ribonuclease inhibitor. TOPP 3 cells transformed with plasmid pTrpmRI6.1 were plated on LB agar plates containing ampicillin (100 μg/mL) and kanamycin (40 μg/mL). A fresh colony was picked within 24 h of transformation, and a starter culture was grown to midlog phase (OD_{600} = 0.5) in LB medium containing ampicillin (200 μg/mL) and kanamycin (40 μg/mL). The starter culture was subjected to centrifugation at 5000*g* for 10 min, and the resulting pellet was suspended in LB medium (25 mL). This suspension was used to inoculate LB medium (3.0 L), containing ampicillin (200 μg/mL) and kanamycin (40 μg/mL). The inoculated culture was shaken (200 rpm) at 37°C until it reached late-log phase (OD_{600} = 1.8). Cells were collected by centrifugation and suspended in Pipes M9 minimal medium (1.0 L) containing ampicillin (200 μg/mL) and kanamycin (40 μg/mL), and shaken (200 rpm) for 10 h at 37°C. The lack of tryptophan in the minimal medium removed repression of the pRI cDNA. The cell suspension was divided into three equal portions. Cells were harvested by centrifugation at 5000*g* for 10 min and frozen in a dry ice/ethanol bath before storage at −80°C. Approximately 15 g of cell paste was obtained from each liter of culture.

A 15-g pellet of frozen cells was thawed by suspending it in 0.50 L of cell lysis buffer, which was 20 mM Tris–HCl buffer (pH 7.8) containing NaCl (0.10 M), EDTA (10 mM), DTT (10 mM), and PMSF (0.04 mM). Cells were lysed on ice by sonication with a Sonifier 450 from Branson Ultrasonics (Danbury, CT) using a duty cycle of 50% and an output control setting of 6. The cell suspension was allowed to cool to 10°C between each of the three 5-min cycles.

To prepare resin for affinity chromatography (34), RNase A (4 mg/mL) was coupled to CNBr-activated Sepharose using the manufacturer's procedures. The resulting RNase A–Sepharose resin had a binding capacity of ≥2 mg of pRI per milliliter of resin. A column (7.0 cm × 1.6 cm^2) of RNase A–Sepharose resin was washed thoroughly with equilibration buffer, which was 50 mM potassium phosphate buffer (pH 6.4) containing DTT (10 mM) and EDTA (1 mM). The cell lysate was subjected to centrifugation at 15,300*g* for 60 min, and the resulting supernatant was loaded onto the column. The loaded column was washed with equilibration buffer (0.30 L), followed by 0.30 L of 50 mM potassium phosphate buffer (pH 6.4) containing NaCl (1.0 M), DTT (10 mM), and EDTA (1 mM). pRI was eluted with 0.10 M sodium acetate buffer (pH 5.0) containing NaCl (3.0 M), DTT (10 mM), and EDTA (1 mM). Fractions were collected and analyzed by SDS–PAGE.

The fractions that contained pRI were combined and dialyzed against 20 mM Tris–HCl buffer (pH 7.5) containing DTT (10 mM) and EDTA (1 mM). The dialysate (0.50 L) was concentrated (to 0.10 L) by ultrafiltration, and any precipitant was removed by centrifugation for 30 min at 15,300*g*. A column (3.0 cm × 0.75 cm^2) of HiTrap Q anion-exchange resin was washed thoroughly with HiTrap Q equilibration buffer, which was 20 mM Tris–HCl buffer (pH 7.5) containing DTT (10 mM) and EDTA (1 mM). The supernatant was loaded onto the column, which had a binding capacity of ≥7 mg of pRI per milliliter of resin. The loaded column was washed with HiTrap Q equilibration buffer (40 mL) and eluted with a linear gradient (80 + 80 mL) of NaCl (0–0.50 M) in equilibration buffer. pRI eluted as a single species at 0.30 M NaCl and was collected and characterized. The purity of pRI was assessed by SDS–PAGE to be >99%. To forestall oxidation of its 30 cysteine residues, solutions of pRI were stored in a tightly capped tube at 4°C in the presence of a reducing agent (5 mM DTT). The protein retained full activity for months under these conditions.

The concentration of active pRI can be determined by titration with RNase A. Accordingly, the ribonucleolytic activity of RNase A was measured in the presence of impure protein during each step of the pRI purification. A solution from each purification step was added to 0.10 M Mes–NaOH buffer (pH 6.0) containing RNase A (12.6 pM), NaCl (0.10 M), and DTT (5 mM) for 5 min at 25°C. The ribonucleolytic activity of an aliquot of this solution was determined by its addition to 0.10 Mes–NaOH buffer (pH 6.0) containing NaCl (0.10 M), DTT (5 mM), and 6-FAM–(dA)rU$(dA)_2$–6-TAMRA (0.60 μM). Kinetic data were analyzed as described previously (29). The units of active pRI during each purification step were determined by using the definition that one unit of RI is the amount of inhibitor required to inhibit the activity of 5 ng of RNase A by 50% (1).

Assays of conformational stability. Differential scanning calorimetry (DSC) was used to determine the conformational stability of RNase A, pRI, and the RI–RNase A complex. The RI–RNase A complex was prepared by adding 1 molar eq of RI to 1.5 molar eq of RNase A and was purified by gel filtration chromatography using a HiLoad 26/60 Superdex 75 column (Amersham Pharmacia Biotech). The RI–RNase A complex and RNase A alone were separated well (data not shown).

DSC experiments were performed as described (35)

TABLE 1

Purification of Recombinant Porcine Ribonuclease Inhibitor[a]

Purification step	Volume (L)	Activity[b] (10^5 units)	Total protein (mg)	Specific activity (units/mg)	Yield (%)	Purification (fold)
Crude lysate supernatant	0.50	8.5	870	977	100	1.0
RNase A–Sepharose affinity chromatography	0.50	5.8	74	7800	68	8.0
HiTrap Q anion-exchange chromatography	0.091	4.4	47	9400	52	9.5

[a] Data are for a 3.0-L culture of TOPP 3 cells (45 g) grown in Luria–Bertani medium.
[b] One unit of ribonuclease inhibitor is the amount required to inhibit the activity of 5 ng of ribonuclease A by 50% (1).

with the following modifications. Protein solutions (0.44–1.24 mg/ml) were dialyzed exhaustively against 0.10 M Mes–NaOH buffer (pH 6.0) containing NaCl (0.10 M) and DTT (5 mM) and then subjected to centrifugation at 15,300*g* for 30 min to remove particulate matter. Data were collected with the program ORIGIN (MicroCal Software; Northampton, MA).

RESULTS AND DISCUSSION

Production and Purification of Ribonuclease Inhibitor

A summary of the purification of pRI from 3 L of *E. coli* culture is shown in Table 1 and Fig. 2. Briefly, cells were harvested by centrifugation and lysed by sonication. The resulting lysate was subjected to centrifugation, and the soluble fraction was loaded onto an RNase A–Sepharose column. The affinity of the RI–RNase A complex is in the femtomolar range (2). This tight interaction was exploited to remove *E. coli* proteins that bind to the RNase A–Sepharose resin by washing with buffer that contained 1.0 M NaCl (1). The pRI that eluted from the RNase A–Sepharose column with buffer that contained 3.0 M NaCl was essentially pure. The RNase A–Sepharose pool produced a single band during SDS–PAGE (Fig. 2; Note: pRI migrates slightly slower than RNasin during SDS–PAGE despite a similar size and net charge). The fractions that contained pRI were collected, dialyzed, and loaded onto an anion-exchange column. The flowthrough contained material that absorbed at 280 nm, but did not contain protein as judged by SDS–PAGE (data not shown). The anion-exchange column was eluted with a linear gradient of NaCl, and pRI eluted as a single species at 0.30 M NaCl. The purity of pRI was judged to be >99% (Fig. 2).

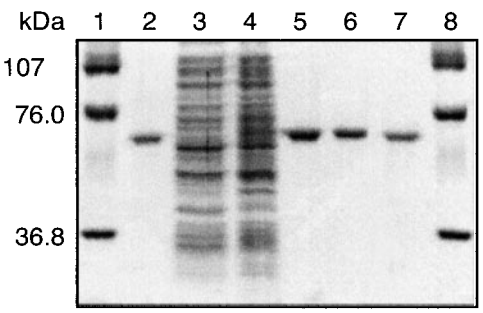

FIG. 2. Expression and purification of recombinant porcine ribonuclease inhibitor from *E. coli* strain TOPP 3 harboring plasmid pTrpmRI6.1. Expression of soluble pRI was performed at 37°C for 10 h. Samples were analyzed by 10% SDS–PAGE. Lane 1, M_r standards: phosphorylase *b* (107 kDa), bovine serum albumin (76.0 kDa), and carbonic anhydrase (36.8 kDa); lane 2, RNasin standard; lane 3, soluble cell lysate before induction; lane 4, soluble cell lysate after inducing for 10 h; lane 5, pooled fractions from RNase A–Sepharose affinity chromatography; lane 6, pooled fractions from HiTrap Q anion-exchange chromatography; lane 7, RNasin standard; lane 8, M_r standards.

Using the *trp* promotor allowed us to produce pRI that was maintained in the cytosol and was soluble during cell lysis. We achieved a yield of approximately 15 mg per liter of culture (1 mg per gram of cell paste). This yield is at least 60-fold greater than any reported previously (22, 28). Such high-level production enables biophysical analysis of RI and its interaction with ribonucleases.

Assays of Conformational Stability

The conformational stability of pRI or its homologs had not been investigated previously. The yield from our expression system enabled us to determine the value of T_m for pRI by differential scanning calorimetry. The unfolding of pRI was irreversible (data not shown). Figure 3A shows the calorimetric scan of pRI in 0.10 M Mes–NaOH buffer (pH 6.0) containing NaCl (0.10 M) and DTT (5 mM). The pRI calorimetric curve contains one peak with a T_m value of 54°C.

In many buffer systems, RNase A unfolds in a reversible two-state process (35, 36). The unfolding of RNase A in the presence of 5 mM DTT was, however, irreversible (data not shown). In addition, the T_m value of RNase A is 59°C in the presence of 5 mM DTT (Fig. 3B) and 62°C in its absence (35, 36). RNase A contains four disulfide bonds with limited solvent accessibility. As the disulfide bonds become exposed to solvent containing DTT, the disulfide bonds undergo reduction. The irreversible unfolding of RNase A can be attributed to the reduction of these disulfide bonds, as the four disulfide bonds of RNase A cannot reoxidize in a buffer

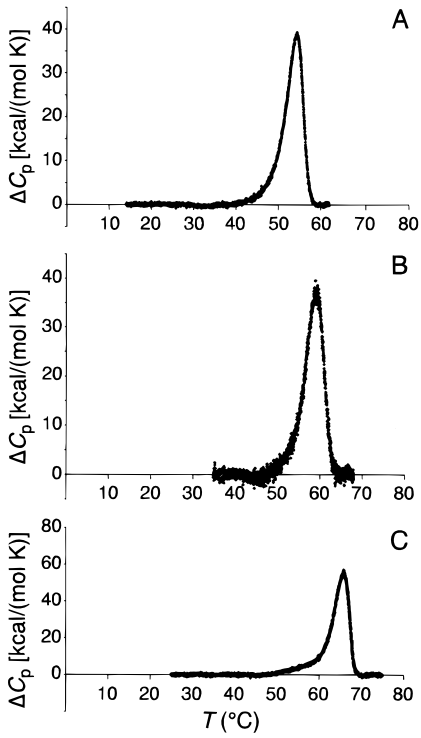

FIG. 3. Differential scanning calorimetry thermal denaturation profiles of (A) porcine ribonuclease inhibitor, (B) ribonuclease A, and (C) the complex of porcine ribonuclease inhibitor and ribonuclease A. Experiments were performed in 0.10 M Mes–NaOH buffer (pH 6.0) containing NaCl (0.10 M) and DTT (5 mM).

system that contains a reducing agent. Accordingly, the presence of DTT lowers the conformational stability of RNase A and, by reducing the disulfide bonds, makes unfolding irreversible.

The calorimetric curve of the pRI–RNase A complex consists of two overlapping peaks with maxima at 61 and 65°C (Fig. 3 C). The minor peak may correspond to the unfolding of unbound RNase A. Each thermal transition of the RI–RNase A complex is higher than the T_m values of its individual components. The major peak is 7 and 12°C greater than the T_m value of RNase A and pRI, respectively.

CONCLUSION

Only low quantities of purified RI were available from previous expression systems. By using the *trp* promoter and producing pRI as a soluble protein in the cytosol of *E. coli*, we achieved a 60-fold greater yield than any obtained previously. This high yield allowed us to perform the first calorimetric experiments on RI and the RI–RNase A complex and will facilitate future structure–function analyses.

ACKNOWLEDGMENTS

This work was supported by Grant CA73808 (NIH). T.A.K. was supported by an Advanced Opportunity Fellowship from the University of Wisconsin–Madison. We thank R. Lowery, D. R. McCaslin, P. Plainkum, and S. M. Fuchs for advice. Calorimetry data were obtained at the University of Wisconsin–Madison Biophysical Instrumentation Facility, which was established by Grants BIR-9512577 (NSF) and S10 RR13790 (NIH) and is supported by the University of Wisconsin–Madison.

REFERENCES

1. Blackburn, P., Wilson, G., and Moore, S. (1977) Ribonuclease inhibitor from human placenta. *J. Biol. Chem*. 252, 5904–5910.
2. Lee, F. S., Shapiro, R., and Vallee, B. L. (1989) Tight-binding inhibition of angiogenin and ribonuclease A by placental ribonuclease inhibitor. *Biochemistry* 28, 225–230.
3. Hofsteenge, J. (1997) Ribonuclease inhibitor *in* "Ribonucleases: Structures and Functions" (D'Alessio, G., and Riordan, J. F., Ed.), pp. 621–658, Academic Press, New York.
4. Lee, F. S., and Vallee, B. L. (1993) Structure and action of mammalian ribonuclease (angiogenin) inhibitor. *Progress Nucleic Acid Res. Mol. Biol.* 44, 1–30.
5. Moenner, M., Vosoghi, M., Ryazantsev, S., and Glitz, D. G. (1998) Ribonuclease inhibitor protein of human erythrocytes: Characterization, loss of activity in response to oxidative stress, and association with Heinz bodies. *Blood Cells Mol. Dis*. 24, 149–164.
6. Raines, R. T. (1998) Ribonuclease A. *Chem. Rev.* 98, 1045–1065.
7. Wu, Y.-N., Saxena, S. K., Wojciech, A., Gadina, M., Mikulski, S. M., De Lorenzo, C., D'Alessio, G., and Youle, R. J. (1995) A study of the intracellular routing of cytotoxic ribonucleases. *J. Biol. Chem*. 270, 17476–17481.
8. Blackburn, P., and Moore, S. (1982) Pancreatic ribonuclease. *Enzymes* 15, 317–433.
9. Vicentini, A. M., Kieffer, B., Matthies, R., Meyhack, B., Hemmings, B. A., Stone, S. R., and Hofsteenge, J. (1990) Protein chemical and kinetic characterization of recombinant porcine ribonuclease inhibitor expressed in *Saccharomyces cerevisiae*. *Biochemistry* 29, 8827–8834.
10. Murthy, B. S., and Sirdeshmukh, R. (1992) Sensitivity of monomeric and dimeric forms of bovine seminal ribonuclease to human placental ribonuclease inhibitor. *Biochem. J.* 281, 343–348.
11. Wu, Y., Mikulski, S. M., Ardelt, W., Rybak, S. M., and Youle, R. J. (1993) A cytotoxic ribonuclease. *J. Biol. Chem*. 268, 10686–10693.
12. Boix, E., Wu, Y.-N., Vasandani, V. M., Saxena, S. K., Ardelt, W., Ladner, J., and Youle, R. J. (1996) Role of the N terminus in RNase A homologues: Differences in catalytic activity, ribonuclease inhibitor interaction and cytotoxicity. *J. Mol. Biol.* 257, 992–1007.
13. Kobe, B., and Deisenhofer, J. (1993) Crystal structure of porcine ribonuclease inhibitor, a protein with leucine-rich repeats. *Nature* 366, 751–756.
14. Hofsteenge, J. (1994) 'Holy' proteins I: Ribonuclease inhibitor. *Curr. Opin. Struct. Biol.* 4, 807–809.
15. Janin, J. (1994) Proteins with a ring. *Structure* 2, 571–573.
16. Kobe, B., and Deisenhofer, J. (1995) A structural basis of the interactions between leucine-rich repeats and protein ligands. *Nature* 374, 183–186.
17. Kobe, B., and Deisenhofer, J. (1995) Proteins with leucine-rich repeats. *Curr. Opin. Struct. Biol.* 5, 409–416.

18. Shapiro, R., Riordan, J. F., and Vallee, B. L. (1995) LRRning the RIte of springs. *Nature Struct. Biol.* 2, 350–354.
19. Kobe, B., and Deisenhofer, J. (1996) Mechanism of ribonuclease inhibition by ribonuclease inhibitor protein based on the crystal structure of its complex with ribonuclease A. *J. Mol. Biol.* 264, 1028–1043.
20. Papageorgiou, A. C., Shapiro, R., and Acharya, K. R. (1997) Molecular recognition of human angiogenin by placental ribonuclease inhibitor—An X-ray crystallographic study at 2.0 Å resolution. *EMBO J.* 16, 5162–5177.
21. Blázquez, M., Fominaya, J. M., and Hofsteenge, J. (1996) Oxidation of sulfhydryl groups of ribonuclease inhibitor in epithelial cells is sufficient for its intracellular degradation. *J. Biol. Chem.* 271, 18638–18642.
22. Kim, B.-M., Schultz, L. W., and Raines, R. T. (1999) Variants of ribonuclease inhibitor that resist oxidation. *Protein Sci.* 8, 430–434.
23. Ui, B. (1971) Isoelectric points and conformation of proteins: The effect of urea on the behavior of some proteins in isoelectric focusing. *Biochim. Biophys. Acta* 229, 567–581.
24. Ardelt, W., Mikulski, S. M., and Shogen, K. (1991) Amino acid sequence of an anti-tumor protein from *Rana pipiens* oocytes and early embryos. *J. Biol. Chem.* 266, 245–251.
25. Kim, J.-S., Soucek, J., Matousek, J., and Raines, R. T. (1995) Mechanism of ribonuclease cytotoxicity. *J. Biol. Chem.* 270, 31097–31102.
26. Chen, C.-Z., and Shapiro, R. (1997) Site-specific mutagenesis reveals differences in the structural bases for tight binding of RNase inhibitor to angiogenin and RNase A. *Proc. Natl. Acad. Sci. USA* 94, 1761–1766.
27. Shapiro, R., Ruiz-Gutierrez, M., and Chen, C.-Z. (2000) Analysis of the interactions of human ribonuclease inhibitor with angiogenin and ribonuclease A by mutagenesis: Importance of inhibitor residues inside versus outside the C-terminal "hot spot." *J. Mol. Biol.* 302, 497–519.
28. Lee, F. S., and Vallee, B. L. (1989) Expression of human placental ribonuclease inhibitor in *Escherichia coli*. *Biochem. Biophys. Res. Commun.* 160, 115–120.
29. Kelemen, B. R., Klink, T. A., Behlke, M. A., Eubanks, S. R., Leland, P. A., and Raines, R. T. (1999) Hypersensitive substrate for ribonucleases. *Nucleic Acids Res.* 27, 3696–3701.
30. Ferreras, M., Gavilanes, J. G., Lopez-Otin, C., and Garcia-Serura, J. M. (1995) Thiol–disulfide exchange of ribonuclease inhibitor bound to ribonuclease A. *J. Biol. Chem.* 270, 28570–28578.
31. Sela, M., Anfinsen, C. B., and Harrington, W. F. (1957) The correlation of ribonuclease activity with specific aspects of tertiary structure. *Biochim. Biophys. Acta* 26, 502–512.
32. Schein, C. H., Boix, E., Haugg, M., Holliger, P., Hemmi, S., Frank, G., and Shwalbe, H. (1992) Secretion of mammalian ribonucleases from *Escherichia coli* using the signal sequence of murine spleen ribonuclease. *Biochem. J.* 283, 137–144.
33. Vicentini, A. M., Hemmings, B. A., and Hofsteenge, J. (1994) Residues 36–42 of liver RNase PL3 contribute to its uridine-preferring substrate specificity: Cloning of the cDNA and site-directed mutagenesis studies. *Protein Sci.* 3, 459–466.
34. Garcia, M. A., and Klebe, R. J. (1997) Affinity chromatography of RNase inhibitor. *Mol. Biol. Rep.* 24, 231–233.
35. Klink, T. A., Woycechowsky, K. J., Taylor, K. M., and Raines, R. T. (2000) Contribution of disulfide bonds to the conformational stability and catalytic activity of ribonuclease A. *Eur. J. Biochem.* 267, 566–572.
36. Klink, T. A., and Raines, R. T. (2000) Conformational stability is a determinant of ribonuclease A cytotoxicity. *J. Biol. Chem.* 275, 1763–17467.
37. Kraulis, P. J. (1991) MOLSCRIPT: A program to produce both detailed and schematic plots of protein structures. *J. Appl. Crystallogr.* 24, 946–950.
38. Merritt, E. A., and Murphy, M. E. P. (1994) Raster3D, Version 2.0, a program for photorealistic molecular graphics. *Acta Crystallogr., Sect. D* 50, 869–873.